

Reduction of a Metal–Organic Framework by an Organometallic Complex: Magnetic Properties and Structure of the Inclusion Compound $[(\eta^5\text{-C}_5\text{H}_5)_2\text{Co}]_{0.5}@\text{MIL-47(V)}^{**}$

Mikhail Meilikhov, Kirill Yusenko, Antonio Torrisi, Bettina Jee, Caroline Mellot-Draznieks, Andreas Pöpl, and Roland A. Fischer*

Probing and fine tuning the physical and chemical properties of metal–organic frameworks (MOFs) by post-synthetic functionalization of the organic linkers is a challenging topic.^[1] For example, redox-inactive MIL-53(Al) can be made redox-active by functionalization of the bridging OH groups of the AlO_6 -type secondary building units (SBUs) of the framework with 1,1'-ferrocenediyl dimethylsilane.^[2] The host–guest chemistry of MOFs (including crystalline porous coordination polymers, PCPs), which exhibit a redox-active framework and in particular involving charge-transfer between the framework and the adsorbed molecules, is an underdeveloped, but very promising area of research.^[3] The few existing reports include the framework oxidation of a nickel(II)-based MOF with I_2 , silver(I), and gold(III) salts.^[4] Furthermore, the partial reduction of MOFs with lithium,^[5] which also involves the aromatic linkers, was discussed to increase the hydrogen uptake.^[6]

Herein, we present the first case of a stoichiometric reduction of the inorganic backbone of a neutral framework in the course of gas-phase loading with an organometallic reducing agent (OMR), and the elucidation of the novel adsorbate structure of the type $[\text{OMR}^+]@[\text{MOF}^-]$.

The adsorption of the volatile OMR cobaltocene, $[(\eta^5\text{-C}_5\text{H}_5)_2\text{Co}]$, in channels of $[\text{VO}(\text{bdc})]$ (MIL-47(V); bdc = 1,4-benzenedicarboxylic acid; MIL = materials of the Institute Lavoisier)^[7a] leads selectively to the inclusion compound of the formula $[(\eta^5\text{-C}_5\text{H}_5)_2\text{Co}]_{0.5}@\text{MIL-47(V)}$ (**1**; Figure 1). The MIL-47(V) network is the isostructural analogue of the well-investigated, redox-inactive phase

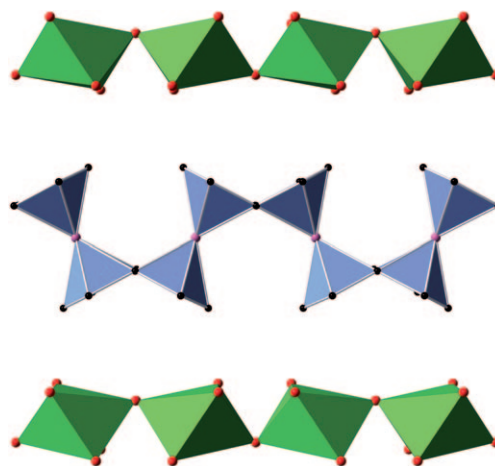


Figure 1. Structure of **1** in the [010] projection. The cobaltocenium occupancy is 50%; that is, only every second position shown is occupied. C black, O red, Co purple; $[\text{VO}_6]$ fragments are displayed as green octahedra.

MIL-53(Al).^[7b] The preparation of **1** was carried out according to previously published procedures for solvent-free loading of MOFs with organometallic compounds.^[8] The elemental analysis of **1** reveals a V/Co ratio of exactly 2:1. The FT-IR spectrum of **1** has a strong vibrational band at 860 cm^{-1} , which is attributed to the formation of cobaltocenium species (Figure 2).

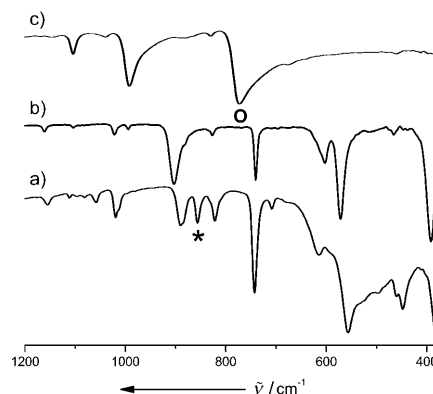


Figure 2. FTIR spectra of **1** (a), activated MIL-47(V) (b), and cobaltocene (c). The characteristic vibrational band of the cobaltocenium ion, $[(\eta^5\text{-C}_5\text{H}_5)_2\text{Co}^+]$, is marked with a star. The vibrational band of cobaltocene is marked with a circle.

[*] M. Meilikhov, Dr. K. Yusenko, Prof. Dr. R. A. Fischer
Lehrstuhl für Anorganische Chemie II
Ruhr-Universität Bochum, 44780 Bochum (Germany)
Fax: (+49) 234-321-4174
E-mail: roland.fischer@ruhr-uni-bochum.de

Dr. A. Torrisi, Dr. C. Mellot-Draznieks
Department of Chemistry, University College London
Gower Street WC1E 6BT, London (United Kingdom)
B. Jee, Prof. Dr. A. Pöpl
Institut für Experimentelle Physik II
Universität Leipzig, 04103 Leipzig (Germany)

[**] We acknowledge financial support from the European Union under the Framework 6 program under a contract for a Specific Targeted Research Project Reference 032109. We would like to acknowledge Dr. E. Bill (MPI für Bioanorganische Chemie, Mülheim) for the magnetic susceptibility study.

Supporting information for this article is available on the WWW under <http://dx.doi.org/10.1002/anie.200907126>.

The absence of any vibrational band in the region 750–790 cm^{-1} indicates that all of the incorporated cobaltocene molecules are oxidized. The vibrational band $\gamma_9(\text{CH})\pi$ is very sensitive to the oxidation state of cobaltocene. In the neutral form of (paramagnetic) cobaltocene, the band appears in the region around 778 cm^{-1} and is shifted to 867 cm^{-1} for the (diamagnetic) cobaltocenium cation.^[9]

The crystal structure of **1** (Figure 1) was solved by a Rietveld analysis of powder X-ray diffraction data (for details, see the Supporting Information). The MIL-47(V) framework is known to be very rigid, in contrast to the breathing nature of MIL-53(Al) that allows large changes of the cell volume ($\pm 470 \text{ \AA}^3$; 33 %). However, the structure of **1** also reveals quite a significant contraction of the cell volume by 120 \AA^3 (9 %) in comparison to the guest-free, activated MIL-47(V). This observation can be explained by the unusually strong host–guest interactions that are due to electrostatic forces between the negatively charged framework and the positively charged cobaltocenium cations. Similar changes of the lattice parameters due to charge transfer are known for related intercalation compounds of cobaltocene inside layered metal phosphorous trisulfides (MPS).^[10] The Co–Cp_{centroid} vectors of **1** are aligned into the *c* axis, with a tilt of about 15° into the channel direction (*a* axis). The orientation only slightly differs from the adsorbate structure of ferrocene inside MIL-53(Al) (**2**), which has ferrocene molecules in a strictly parallel orientation of the Fe–Cp_{centroid} vectors.^[8] The C₅H₅ rings of **2** are coplanar to the O₃Al faces of the AlO₆ octahedra, which point towards the channel.^[11] The occupancy of the cobaltocene positions of **1** is only 50 %, which means that only every second cobaltocenium position shown in Figure 1 is occupied. Nevertheless, the packing of the cobaltocenium cations of **1** is as dense as in case of **2**.^[8] The importance of the framework reduction of **1** for guest adsorption is clearly illustrated by the much lower uptake of metallocene and the quite different adsorbate structure of $[(\eta^5\text{-C}_5\text{H}_5)_2\text{Fe}]_{0.25}\text{@MIL-47(V)}$ (**3**; Supporting Information, Figure S4) as compared with **1** and **2**.

The framework reduction was supported by electron spin resonance (ESR) measurements. In the pure MIL-47(V), the signal of an $S = 1/2$ spin system is observed with an anisotropic *g* factor corresponding to a d¹ V^{IV} ion. The principal values are $g_{xx,yy} = 1.969$ and $g_{zz} = 1.943$. The axial *g* tensor revealed a distorted octahedral environment (axially compressed) for

the V atom, as expected in MIL-47(V).^[12] There is no ⁵¹V hyperfine structure observed due to spin-exchange effects caused by the high-spin concentration in the magnetically undiluted material. In the ESR spectrum of **1** (Figure 3), the strong signal of the $S = 1/2$ spin system of MIL-47(V) is absent, and only a very weak signal is observed. Detailed analysis of the weak signal in the spectrum of **1** (Supporting Information, Figure S9) shows the signal of a $S = 1/2$ spin system with a well-resolved ⁵¹V hyperfine structure with axially symmetric *g* and *A* tensors ($g_{xx}, g_{yy} = 1.979$, $g_{zz} = 1.941$, $A_{xx}, A_{yy} = 0.0062 \text{ cm}^{-1}$, $A_{zz} = 0.0172 \text{ cm}^{-1}$), which is also present in the activated pure MIL-47(V) starting material (Supporting Information, Figure S9) and therefore is assigned to isolated extraframework V^{IV} impurities. This V^{IV} ESR signal is superimposed on a broad background signal with a *g* value of $g = 1.96$, which is most likely due to clustered paramagnetic vanadium species and rules out Co^{III} species. The ESR parameters could be determined by simulation using the EasySpin ESR simulation package.^[13] The analysis of magnetic susceptibility measurement reveals an antiferromagnetic behavior of **1**, with a Néel temperature of 100 K (Figure 3). The fit of the linear (paramagnetic) part of the $1/\chi$ curve follows a Curie–Weiss law. The experimental effective magnetic momentum for **1** is $\mu_{\text{eff}} = 2.45 \mu_B$. The expected spin-only magnetic moment is $2.83 \mu_B$ for V^{III} and $1.73 \mu_B$ for V^{IV}.^[12] For a 1:1 V^{III}/V^{IV} system the calculated magnetic moment is $2.36 \mu_B$. The agreement of the calculated and experimentally observed magnetic moments confirms the assignment of a stoichiometric mixed-valence framework. The obtained differential pulse voltammetry (DPV) data of **1** shows a shift of 0.33 V of the main maximum to the lower potential and the appearance of a second new maximum compared to that of activated, empty MIL-47(V) (Figure 3). Both phenomena can be explained by the mixed-valence framework. The redox-potential of the couple cobaltocenium/cobaltocene is much more negative and out of the range of the measurement ($E^\circ \approx -1.3 \text{ V}$).^[14]

To better understand the electronic state of **1**, we performed DFT single-point energy calculations. The PW91 functional was used in conjunction with DNP (double numerical plus polarization) basis set. A three-dimensional model of the MIL-47(V^{IV}/V^{III}) structure was used, which considers three different spin alignments for each system corresponding to ferromagnetic, ferrimagnetic, and antiferromagnetic configurations (A, B, and C in the Supporting

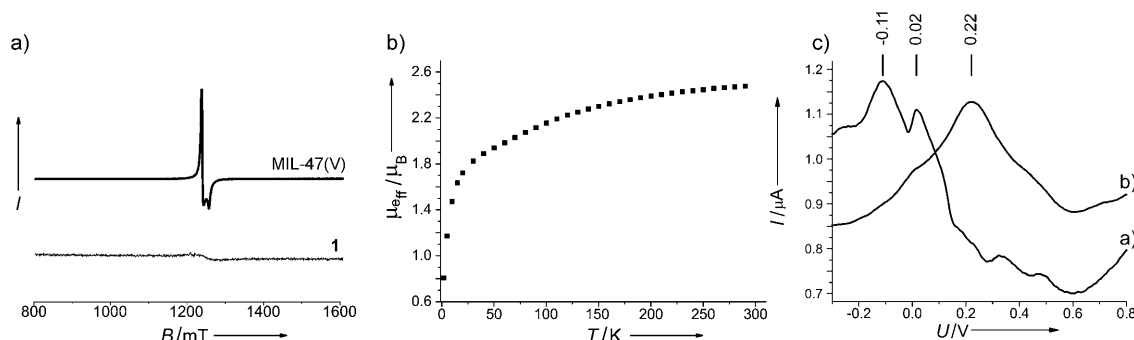


Figure 3. a) cw ESR spectra of **1** and activated MIL-47(V) ($\nu_{\text{mw}} = 34 \text{ GHz}$, $T = 9 \text{ K}$). The ESR spectrum of **1** is shown with a tenfold magnification. b) The molar magnetic susceptibility of **1** as a function of temperature. c) Differential pulse voltammetry of **1** and activated MIL-47(V).

Information, Figure S12). The calculations were performed with a 321 K point sampling (see the Supporting Information for details). The calculations indicate the antiferromagnetic configuration as that with the lowest energy and consequently as the thermodynamically most favorable. The spin population analysis seems to indicate two important factors as main reasons of the thermodynamic stabilization of the system: The first is the spin delocalization on the two metal cations with different valence, and the second is the antiparallel alignment between the chains. These two factors make the antiferromagnetic configuration that with the highest thermodynamic stability (Figure 4). Interestingly, related calculations on the magnetic properties of MIL-53(Cr) gave an equally good qualitative agreement with the experimental values, and the antiferromagnetic phase was also found to be the most stable.^[15]

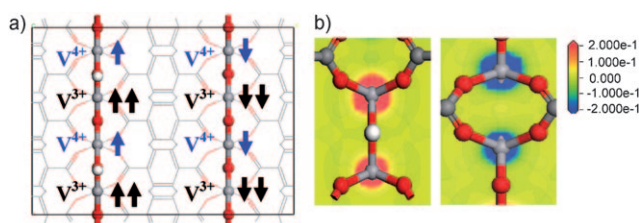


Figure 4. a) Representation of the antiferromagnetic spin configuration of 3D-MIL-47(V^{IV}/V^{III}). b) Snapshot of the spin density for the antiferromagnetic spin configuration of 3D-MIL-47(V^{IV}/V^{III}). The single-point energy calculation was performed with the PW91/DNP method.^[16]

The irreversible adsorption of cobaltocene and the unusually strong binding of the cobaltocenium guest to the host framework are also shown by the thermal gravimetric data (TG, see the Supporting Information). There is no weight loss (that is, no desorption of cobaltocene) below the decomposition temperature of MIL-47(V) ($T = 420^\circ\text{C}$). This behavior is in contrast to the related inclusion compound $[(\eta^5\text{-C}_5\text{H}_5)_2\text{Fe}]_{0.5}@\text{MIL-53(Al)}$ (**2**).^[8] Quantitative desorption of ferrocene, $[(\eta^5\text{-C}_5\text{H}_5)_2\text{Fe}]$, takes place between 250 and 450°C , which is much below decomposition of the framework. Quite obviously, electrostatic forces substantially contribute to the binding of cobaltocene inside the partially reduced MIL-47(V) framework. Co-adsorption experiments were performed using equimolar mixtures of both metallocenes, and the results were compared to similar co-adsorption experiments with MIL-53(Al). The elemental analysis and thermal gravimetry data show preferred uptake of cobaltocene over ferrocene of 2:1 for MIL-47(V). In contrast, MIL-53(Al) shows the reversed selectivity of 1:2, with a preference for ferrocene. The driving force of the selectivity of MIL-47(V) is the charge transfer between the host framework and the guest molecule, which also induces unusual framework flexibility.

Finally, the obvious issue of releasing the cobaltocenium guest from **1** should be mentioned. Simple washing with water under an argon atmosphere leads to a material with a PXRD pattern very similar to the hydrated phase of MIL-47(V), but with a slightly reduced cell volume. The UV/Vis data of the aqueous washing solution is identical to a cobaltocenium salt

reference sample. However, re-oxidation of V^{III} to V^{IV} in an aqueous medium under these conditions is difficult to rule out. Further investigations of selective cation exchange reactions and keeping the mixed-valence state of the framework unchanged are underway. The transfer of the concept to iron(III)- and chromium(III)-containing frameworks that are redox-active and isostructural with MIL-53 is in progress as well.

In summary, we have demonstrated a novel concept for stoichiometric reduction of the redox-active framework metal ions of a typical MOF, yielding a well-defined mixed-valence material by incorporation of a suitable organometallic reducing agent. The oxidized form of this reductant is chemically inert and does not interfere with the overall coordination chemistry and stability of the MOF. The redox potential of organometallic reductants can be fine-tuned by substituent effects. The combination of co-adsorption with other redox-inactive guests under solvent-free conditions and subsequent cation exchange may offer unique possibilities of adjusting the mixed-valence states of redox-active frameworks.

Experimental Section

1: A sample of MIL-47(V) (50 mg, 0.22 mmol) was placed together with CoCp₂ (100 mg, 0.53 mmol, 2.5 equiv) in separate small glass vessels in a Schlenk tube. After reducing the pressure to 10^{-3} mbar at room temperature and sealing under static vacuum, the reaction tube was heated to 40°C for 72 h. During this treatment, the yellow/green MIL-47(V) powder turned black. Yield: 95 mg.

Crystal data of **1**: space group *Imma* (no 74); $a = 6.711(2)$, $b = 18.743(3)$, $c = 10.281(2)$ Å, $V = 1293.1(5)$ Å³; $Z = 4$; $R_p = 0.021$, $R_{wp} = 0.027$, $R_b = 0.13$, $1/2\text{Co}$ ($1/4$ $1/4$ $1/4$). All details of crystal structure solution and refinement can be found in the Supporting Information. CCDC 757792 contains the supplementary crystallographic data for this paper. These data can be obtained free of charge from The Cambridge Crystallographic Data Centre via www.ccdc.cam.ac.uk/data_request/cif.

Details of the co-adsorption experiments, IR and UV/Vis spectroscopy, ESR, differential pulse voltammetry, elemental analysis, and thermal analysis of **1** are described in the Supporting Information.

Received: December 17, 2009

Revised: March 16, 2010

Published online: July 22, 2010

Keywords: breathing effect · charge-transfer · coordination polymers · inclusion compounds · metal–organic frameworks

- [1] a) Z. Wang, S. Cohen, *Chem. Soc. Rev.* **2009**, 38, 1315–1329; b) C. J. Doonan, W. Morris, H. Furukawa, O. M. Yaghi, *J. Am. Chem. Soc.* **2009**, 131, 9492–9493; c) T. Gadzikwa, O. K. Farha, C. D. Malliakas, M. G. Kanatzidis, J. T. Hupp, S. T. Nguyen, *J. Am. Chem. Soc.* **2009**, 131, 13613–13615.
- [2] M. Meilikhov, K. Yusenko, R. A. Fischer, *J. Am. Chem. Soc.* **2009**, 131, 9644–9645.
- [3] a) S. Kitagawa, R. Matsuda, *Coord. Chem. Rev.* **2007**, 251, 2490–2509.
- [4] a) H. J. Choi, M. P. Suh, *J. Am. Chem. Soc.* **2004**, 126, 15844–15851; b) M. P. Suh, H. R. Moon, E. Y. Lee, S. Y. Jang, *J. Am.*

- Chem. Soc.* **2006**, *128*, 4710–4718; c) H. R. Moon, J. H. Kim, M. P. Suh, *Angew. Chem.* **2005**, *117*, 1287–1291; *Angew. Chem. Int. Ed.* **2005**, *44*, 1261–1265.
- [5] a) G. Férey, F. Millange, M. Morcrette, C. Serre, M.-L. Doublet, J.-M. Grenèche, J.-M. Tarascon, *Angew. Chem.* **2007**, *119*, 3323–3327; *Angew. Chem. Int. Ed.* **2007**, *46*, 3259–3263; b) K. L. Mulfort, J. T. Hupp, *J. Am. Chem. Soc.* **2007**, *129*, 9604–9605; c) K. L. Mulfort, J. T. Hupp, *Inorg. Chem.* **2008**, *47*, 7936–7938; d) K. L. Mulfort, T. M. Wilson, M. R. Wasielewski, J. T. Hupp, *Langmuir* **2009**, *25*, 503–508.
- [6] D. Himsl, D. Wallacher, M. Hartmann, *Angew. Chem.* **2009**, *121*, 4710–4714; *Angew. Chem. Int. Ed.* **2009**, *48*, 4639–4642.
- [7] a) K. Barthelet, J. Marrot, D. Riou, G. Férey, *Angew. Chem.* **2002**, *114*, 291–294; *Angew. Chem. Int. Ed.* **2002**, *41*, 281–284; b) T. Loiseau, C. Serre, C. Huguenard, G. Fink, F. Taulelle, M. Henry, T. Bataille, G. Férey, *Chem. Eur. J.* **2004**, *10*, 1373–1382.
- [8] a) M. Meilikhov, K. Yushenko, R. A. Fischer, *Dalton Trans.* **2009**, 600–602; b) H. Kim, H. Chun, G. H. Kim, H. S. Lee, K. Kim, *Chem. Commun.* **2006**, 2759–2761.
- [9] H. P. Fritz, *Adv. Organomet. Chem.* **1964**, *1*, 239–316.
- [10] a) R. Clement, M. L. H. Green, *J. Chem. Soc. Dalton Trans.* **1979**, 1566–1568; b) D. G. Clerc, D. A. Cleary, *Chem. Mater.* **1992**, *4*, 1344–1348.
- [11] K. Barthelet, K. Adil, F. Millange, C. Serre, D. Riou, G. Férey, *J. Mater. Chem.* **2003**, *13*, 2208–2212.
- [12] a) D. Kivelson, S.-K. Lee, *J. Chem. Phys.* **1964**, *41*, 1896–1903; b) R. Gallay, J. J. van der Klink, J. Moser, *Phys. Rev. B* **1986**, *34*, 3060–3068.
- [13] S. Stoll, A. Schweiger, *J. Magn. Reson.* **2006**, *178*, 42–55.
- [14] N. G. Connelly, W. E. Geiger, *Chem. Rev.* **1996**, *96*, 877–910.
- [15] D. S. Coombes, F. Corà, C. Mellot-Draznieks, R. G. Bell, *Chem. Phys.* **1991**, *94*, 7245–7250.
- [16] a) B. J. Delley, *Chem. Phys.* **1991**, *94*, 7245–7250; b) J. P. Perdew, J. A. Chevary, S. H. Vosko, K. A. Jackson, M. R. Pederson, D. J. Singh, C. Fiolhais, *Phys. Rev. B* **1992**, *46*, 6671–6687.